Proceedings of DETC'06:
30th Annual Mechanisms and Robotics Conference
September 10-13, 2006; Philadelphia, PA

DETC2006-99243

FINITE ELEMENT MODELING OF COUPLED FLEXIBLE MULTIBODY DYNAMICS AND LIQUID SLOSHING

Tamer M. Wasfy
Advanced Science and Automation Corp., Indianapolis, IN

ABSTRACT

A time-accurate finite element model for simulating the fully-coupled dynamic response of flexible multibody systems and liquid sloshing in tanks is presented. The semi-discrete combined solid and fluid equations of motions are integrated using a time-accurate parallel explicit solver. The FE model consists of: hexahedral, beam, and truss solid elements; rigid bodies; joints; actuators; hexahedral incompressible fluid elements; and quadrilateral fluid-solid interface elements. The fluid mesh is modeled using a very light and compliant solid mesh which allows the fluid mesh to move/deform along with the tank using the Arbitrary Lagrangian-Eulerian formulation. The fluid's free-surface is modeled using an acceptor-donor volume-of-fluid based algorithm. The motion of the solid and fluid is referred to a global inertial Cartesian reference frame. A total Lagrangian deformation description is used for the solid elements. The penalty technique is used to model the joints. Numerical simulations are presented for a half-filled tank supported by linear springs mounted on a test fixture.

1. INTRODUCTION

Many practical applications include a flexible multibody system carrying liquid filled tanks. The multibody system can be a ground vehicle (truck, train, or car), ship, airplane (commercial or military jet, helicopter, etc.), or a space structure (space station or satellite). The tank can be a payload tank or a liquid fuel tank. Optimum system design in those applications requires an accurate computational model of the system response, which in turn requires accurate modeling of the following:

- Incompressible fluid flow in a moving/deforming container including accurate modeling of the free-surface, turbulence, and viscous effects.
- Flexible multibody system, including: flexible bodies, rigid bodies, joints, frictional contact.
- Coupling between the solid and the fluid at the fluid-structure interface.

The fluid flow is governed by the incompressible Navier-Stokes equations. Finite volume [1, 2, 3], finite element [4, 5, 6] or particle [7] discretization techniques have been used to model the fluid flow. In addition, many techniques for modeling fluid flow with a free-surface in a moving/deforming container have been developed in the literature, these include:

(a) *Fixed Cartesian fluid mesh with volume-of-fluid (VOF) free-surface model.* The fluid domain is a Cartesian mesh. The container moves inside this mesh. Therefore, a cut-cell technique must be used in order to find where the boundary of the container intersects with the fluid cells. The cut-cell surfaces are then used to impose wall impenetrability and adhesion boundary conditions [1, 2]. A VOF technique [8, 9] is used to model the liquid free-surface where each element has a VOF value between 0 (for empty elements) and 1 (for elements completely filled with fluid). The free surface is reconstructed for each element using piecewise-linear planar segments using the VOF value of the element along with the VOF values of neighboring elements (which are used to determine the normal to the planar surface). Note that when VOF algorithms were first used the free surface was reconstructed using either vertical or horizontal surfaces [8, 3]. The VOF values of all the elements are updated each time step by calculating the mass flux between elements. The mass flux for free-surface elements is calculated by taking into account the smaller surface through which the fluid can move due to the presence of the free surface. The fixed Cartesian mesh with VOF technique has the advantage that mesh generation is straightforward. Also, the technique can easily deal with floating objects and tank baffles. However, the disadvantage of the technique is that the fluid-solid impenetrability and no-slip boundary conditions are satisfied only in a time average sense. Also, the method has stability and accuracy problems when the cut-cell elements at the solid-fluid interface become small.

(b) *Moving ALE mesh.* The fluid is modeled using a fluid mesh that moves and deforms with the tank as well as with the fluid's free-surface using the ALE formulation [4, 6, 10]. The main disadvantage of this method is that it does not allow large surface deformation including surface break-up and merging unless the fluid domain is re-meshed [11, 12]. If re-meshing is used frequently, then there is the problem of degraded solution accuracy due to re-interpolation of the solution field onto the new mesh.

Report Documentation Page

Form Approved
OMB No. 0704-0188

1. REPORT DATE	2. REPORT TYPE	3. DATES COVERED
11 SEP 2006	**Journal Article**	**11-09-2006 to 11-09-2006**

4. TITLE AND SUBTITLE
FINITE ELEMENT MODELING OF COUPLED FLEXIBLE MULTIBODY DYNAMICS AND LIQUID SLOSHING

5a. CONTRACT NUMBER
W56HZV -05-C-0117

5b. GRANT NUMBER

5c. PROGRAM ELEMENT NUMBER

6. AUTHOR(S)
Tamer Wasfy

5d. PROJECT NUMBER

5e. TASK NUMBER

5f. WORK UNIT NUMBER

7. PERFORMING ORGANIZATION NAME(S) AND ADDRESS(ES)
U.S. Army TARDEC ,6501 E.11 Mile Rd,Warren,MI,48397-5000

8. PERFORMING ORGANIZATION REPORT NUMBER
#15854

9. SPONSORING/MONITORING AGENCY NAME(S) AND ADDRESS(ES)
U.S. Army TARDEC, 6501 E.11 Mile Rd, Warren, MI, 48397-5000

10. SPONSOR/MONITOR'S ACRONYM(S)
TARDEC

11. SPONSOR/MONITOR'S REPORT NUMBER(S)
#15854

12. DISTRIBUTION/AVAILABILITY STATEMENT
Approved for public release; distribution unlimited

13. SUPPLEMENTARY NOTES
Contract company is Advanced Science and Automation Corp., Indianapolis, IN Submitted to 30TH ANNUAL MECHANISMS AND ROBOTICS CONF - SEPT 10-13 06 PHILADELPHIA, PA

14. ABSTRACT

A time-accurate finite element model for simulating the fullycoupled dynamic response of flexible multibody systems and liquid sloshing in tanks is presented. The semi-discrete combined solid and fluid equations of motions are integrated using a time-accurate parallel explicit solver. The FE model consists of: hexahedral, beam, and truss solid elements; rigid bodies; joints; actuators; hexahedral incompressible fluid elements; and quadrilateral fluid-solid interface elements. The fluid mesh is modeled using a very light and compliant solid mesh which allows the fluid mesh to move/deform along with the tank using the Arbitrary Lagrangian-Eulerian formulation. The fluid's free-surface is modeled using an acceptor-donor volume-of-fluid based algorithm. The motion of the solid and fluid is referred to a global inertial Cartesian reference frame. A total Lagrangian deformation description is used for the solid elements. The penalty technique is used to model the joints. Numerical simulations are presented for a half-filled tank supported by linear springs mounted on a test fixture.

15. SUBJECT TERMS

16. SECURITY CLASSIFICATION OF:			17. LIMITATION OF ABSTRACT	18. NUMBER OF PAGES	19a. NAME OF RESPONSIBLE PERSON
a. REPORT	b. ABSTRACT	c. THIS PAGE			
unclassified	**unclassified**	**unclassified**	**Same as Report (SAR)**	**9**	

(c) Fixed-fluid mesh with the Navier-Stokes equations written in a reference frame fixed to the tank along with a VOF free-surface model [4, 13].

(d) *Moving ALE mesh with a VOF free-surface model.* The fluid domain is modeled using a mesh that moves and deforms with the tank. Then the VOF technique outlined above is used to model the liquid free-surface. This method does not suffer from the cut-cell solid-fluid interface boundary-condition problem like method (a). It also allows modeling surface break-up and merging without the need for re-meshing. This is the method that is used in the present paper.

(e) *Moving ALE mesh with a level-set free-surface model* [5]. This method is the same as method (d) except that a level-set method is used to model the liquid free surface. The method uses a smooth scalar function defined at every point in the fluid domain which specifies the signed smallest Eucledian distance between the point and the interface. The evolution of the scalar function is governed by a convection transport equation where the interface is moved with the fluid velocity.

(f) *Lagrangian Particle methods.* Lagrangian particles are used to model the fluid. A contact model between the fluid particles and the tank is used to model the fluid-structure interaction. The main disadvantage of those types of methods is the large number of particles and computing time needed to accurately predict the fluid motion. A special type of this class of methods which has been successfully applied to fluid-structure interaction problems is the particle finite element method (PFEM) [6] in which the particles are used to generate a polyhedral finite element mesh every time step using an extended Delaunay tesselation. The solution of the incompressible Navier-Stokes equations is then carried using that mesh. The PFEM requires less fluid particles, however, the tessellation step is computationally intensive. Particle methods can easily handle surface break-up and merging, floating bodies, and fluid-solid impenetrability boundary condition.

A review of multibody dynamics modeling techniques including deformation reference frames, treatment of large rotations, discretization techniques, finite elements, constraint and contact modeling, and solution techniques is presented in [14]. Flexible multibody systems involving liquid filled tanks are generally ground, marine, air, or space vehicles where the following need to be accurately modeled:

- Large arbitrary rigid body translation and rotation.
- Rigid bodies.
- Flexible bodies which can be composed of beam, shell or solid elements. Those include for example a shell model for a flexible tank.
- Joints including spherical, revolute, prismatic, and universal joints. Joint friction and clearances also need to be modeled.
- Frictional contact. For example for ground vehicle applications the rolling frictional contact of tires need to be accurately modeled.
- Transmission components, clutches, and brakes for ground vehicle applications. All those components involve friction.

In order to satisfy the above requirements a flexible multibody dynamics modeling technique with the following characteristics is used:

- An explicit time-integration solver accurate for long simulation times [15].
- Total Lagrangian, total displacement equations of motion formulation with the degrees of freedom referred to a global inertial reference frame [15, 16, 17, 18].
- A library of truss, beam, and solid nonlinear finite elements with Cartesian coordinate degrees of freedom allowing arbitrarily large element rotations. Those include:
  - Torsional-spring type 3-node beam elements [15, 16].
  - Natural-modes eight-node brick elements [17, 18]. Those elements can also be used to model shells and beams. One element through the thickness is sufficient to accurately model the membrane, shear, and bending characteristics. They do not exhibit locking or spurious modes (widely used techniques to alleviate locking such as hourglass control lead to elements that do not maintain solution accuracy over very long solution times). They are computationally efficient. Assumed strain elements of comparable accuracy are more computationally expensive. Any material law can be used with those elements including: linear elastic, hyper-elastic, and non-linear laws.
- Penalty formulation for modeling joints (spherical, revolute, cylindrical and prismatic) [19].
- Rigid body rotational equations of motion are written in a body (material) frame, with the resulting incremental rotations added to the total body rotation matrix [19].
- Normal contact modeled using a penalty formulation [20, 21].
- Frictional contact modeled using an accurate and efficient asperity-based friction model [22].
- Special elements for modeling wheels/pulleys [20], sprockets [23], and clutches [24].
- General tire model [21]. The model includes the details of the tire construction. The tire rubber is modeled using brick elements. The bead, tread and ply are modeled using beam elements along the tire circumference and meridian directions with appropriate stiffness and damping properties. Normal contact between the tire and the wheel and between the tire and the pavement is modeled using the penalty technique. Friction is modeled using an asperity-based approximate Coulomb friction model. The tire inflation pressure is modeled by applying a force normal to the inner surface elements of the tire with the out-of-equilibrium force and moment applied to the wheel to guarantee self-equilibrium of the tire and wheel under the pressure load [21].
- General contact search algorithm that find the contact penetration between finite elements and other elements as well as general triangle and quadrilateral surfaces.

Two-way coupling between the multibody system (vehicle) motion and the fluid is achieved by satisfying the following conditions at the solid-fluid interface:

- The fluid velocity normal to the solid's surface must be equal to the normal solid velocity.

- The fluid velocity tangent to the solid surface can range from being equal to the tangential velocity of the solid surface (no slip condition) to being free.
- No additional energy or momentum to the system should be introduced at the interface.

The proper boundary condition that does not violate the above conditions arises from the use of Newton's equations of motion to find a common normal acceleration for the fluid and the solid at the interface. The tangential fluid and solid accelerations can range from being the same (no-slip condition) to being completely decoupled.

Finally in the present paper, a single computational code which uses a time-accurate explicit solution procedure is used to solve both the solid and fluid equations of motion. Many commercial software and studies on modeling liquid sloshing coupled with solid body motion use two codes which pass the interface forces and motion back and forth and iterate on the two codes until equilibrium is achieved [e.g. 3, 13]. This approach adds additional computational burden and does not achieve the same accuracy as the single integrated code solution.

The rest of this paper is organized as follows. In Sections 2 and 3 the equations of motion for the solid and fluid are presented. In Section 4 the fluid-structure coupling model is presented. In Section 5 the VOF free-surface model is presented. In Section 6 the overall explicit solution procedure is outlined. In Section 7 numerical simulations of a multibody test fixture with a liquid filled tank are presented. Finally, in Section 8 some concluding remarks are offered.

2. SOLID EQUATIONS OF MOTION

In the subsequent equations the following conventions will be used:

- The indicial notation is used.
- The Einstein summation convention is used for repeated subscript indices unless otherwise noted.
- Upper case subscript indices denote node numbers.
- Lower case subscript indices denote vector component number.
- The superscript denotes time.
- A superposed dot denotes a time derivative.

The translational equations of motion are written with respect to the global inertial reference frame and are obtained by assembling the element equations. The finite elements used here use only translational DOFs with no rotational DOFs. This is advantageous in terms of computational efficiency, accuracy, and robustness [14]. Those equation also include the rigid-body (such as the wheel) translational DOFs. The equations can be written as:

$$M_K \ddot{x}^t_{Ki} = F_{s}{}^t_{Ki} + F_{a}{}^t_{Ki} \qquad (1)$$

where t is the running time, K is the global node number (no summation over K; K=1→N where N is the total number of nodes), i is the coordinate number (i=1,2,3), a superposed dot indicates a time derivative, M_K is the lumped mass of node K, x is the vector of nodal Cartesian coordinates with respect to the global inertial reference frame, and $\ddot{x}$ is the vector of nodal accelerations with respect to the global inertial reference frame, F_s is the vector of internal structural forces, and F_a is the vector of externally applied forces, which include surface forces and body forces.

For each rigid body, a body-fixed material frame is defined. The rigid body is represented by one node located at the body's center of mass, which is also the origin of this frame. The mass of the body is concentrated at the node and the inertia of the body given by the inertia tensor I_{ij} defined with respect to the body frame. The orientation of the body-frame is given by $R^{t_0}_K$ which is the rotation matrix relative to the global inertial frame at time t_0. The rotational equations of motions are written for each rigid body with respect to its body-fixed material frames as:

$$I_{Kij}\ddot{\theta}^t_{Kj} = T_{s}{}^t_{Ki} + T_{a}{}^t_{Ki} - \left(\dot{\theta}^t_{Ki} \times (I_{Kij}\dot{\theta}^t_{Kj})\right)_{Ki} \qquad (2)$$

where I_K is the inertia tensor of rigid body K, $\ddot{\theta}_{Kj}$ and $\dot{\theta}_{Kj}$ are the angular acceleration and velocity vectors' components for rigid body K relative to it's material frame in direction j, Ts_{Ki} are the components of the vector of internal torque at node K in direction i, and Ta_{Ki} are the components of the vector of applied torque. The summation convention is used only for the lower case indices i and j.

The trapezoidal rule is used as the time integration formula for solving equations (1) for the global nodal positions x:

$$\dot{x}^t_{Kj} = \dot{x}^{t-\Delta t}_{Kj} + 0.5\,\Delta t\,(\ddot{x}^t_{Kj} + \ddot{x}^{t-\Delta t}_{Kj}) \qquad (3a)$$

$$x^t_{Kj} = x^{t-\Delta t}_{Kj} + 0.5\,\Delta t\,(\dot{x}^t_{Kj} + \dot{x}^{t-\Delta t}_{Kj}) \qquad (3b)$$

where Δt is the time step. The trapezoidal rule is also used as the time integration formula for the nodal rotation increments:

$$\dot{\theta}^t_{Kj} = \dot{\theta}^{t-\Delta t}_{Kj} + 0.5\,\Delta t\,(\ddot{\theta}^t_{Kj} + \ddot{\theta}^{t-\Delta t}_{Kj}) \qquad (4a)$$

$$\Delta\theta^t_{Kj} = 0.5\,\Delta t\,(\dot{\theta}^t_{Kj} + \dot{\theta}^{t-\Delta t}_{Kj}) \qquad (4b)$$

where $\Delta\theta_{Kj}$ are the incremental rotation angles around the three body axes for body K. The rotation matrix of body K (R_K) is then evaluated using:

$$R^t_K = R^{t-\Delta t}_K\, R(\Delta\theta^t_{Ki}) \qquad (5)$$

where $R(\Delta\theta^t_{Ki})$ is the rotation matrix corresponding to the incremental rotation angles from Equation (4b).

The explicit solution procedure used for solving equations (1-5) along with constraint equations is presented in Section 6. The constraint equations are generally algebraic equations, which describe the position or velocity of some of the nodes. They include:

- Prescribed motion constraints:
$$f(\{x\},t) = 0 \qquad (6)$$
- Joint constraints:
$$f(\{x\}) = 0 \qquad (7)$$
- Contact/impact constraints:
$$f(\{x\}) \geq 0 \qquad (8)$$

The penalty technique is used for imposing the constraints in which a normal reaction force is generated when a node is penetrates in a contact body whose magnitude is proportional to the penetration distance [20, 21]. An asperity-spring friction model is used to model joint and contact friction [22] in which friction is modeled using a piece-wise linear velocity-dependent approximate Coulomb friction element in parallel with a

variable anchor point spring. The model approximates asperity friction where friction forces between two rough surfaces in contact arises due to the interaction of the surface asperities.

3. SEMI-DISCRETE FLUID EQUATIONS OF MOTION

The dynamic response of the fluid is described by the ALE version of the incompressible Navier-Stokes equations, namely, the equations of conservation of momentum and mass for a moving deforming control volume: which are:

$$\int_V \rho \frac{\partial u_i}{\partial t} dV = \int_V -u_i \frac{\partial \rho}{\partial t} dV + \int_V \frac{\partial [-\rho u_i \hat{u}_j - P\delta_{ij} + \tau_{ij}]}{\partial x_j} dV + \int_V \rho f_i dV \quad (9)$$

$$\int_V \frac{\partial \rho}{\partial t} dV + \int_V \frac{\partial (\rho \hat{u}_i)}{\partial x_i} dV = 0 \quad (10)$$

$$\rho = \rho_0 + r\,P \quad (11)$$

$$\hat{u}_i = u_i - v_i \quad (12)$$

$$\tau_{ij} = \lambda D_{kk}\delta_{ij} + 2(\mu + \mu_t + \mu_s)D_{ij} \quad (13a)$$

$$D_{ij} = 0.5\left(\partial \hat{u}_i / \partial x_j + \partial \hat{u}_j / \partial x_i\right) \quad (13b)$$

where V is the element volume, t is the running time, ρ is the density of the fluid, $\vec{u}$ is the fluid velocity vector relative to the global reference frame, $\vec{\hat{u}}$ is the fluid velocity vector relative to the moving fluid mesh, $\vec{v}$ is the velocity of the fluid mesh, P is the relative pressure, $\vec{x}$ is the position vector, τ is the deviatoric stress tensor, D is the rate of deformation tensor, $\vec{f}$ is the body force vector, r is the artificial compressibility parameter, ρ_0 is the nominal fluid density, μ is the fluid viscosity, μ_t is an additional turbulence viscosity (set proportional to vorticity magnitude), and μ_s is an additional free-surface viscosity used to model the interaction between the liquid and the gas that is above it. Incompressible flow is modeled using the artificial compressibility technique [25]. A finite element formulation is used to derive the element's semi-discrete equations of motion from the governing equations (9-13). 8-node hexahedral elements are used with tri-linear equal-order velocity and pressure interpolation. A pressure averaging algorithm [26] is used to eliminate pressure checker-boarding (due to the use of an equal order interpolation for pressure and velocity). The element equations are assembled into the global semi-discrete equations of motion:

$$M_{f_K}\,\dot{u}^t_{Ki} = F^t_{f_{Ki}} \quad (14)$$

$$V_{f_K}\,\dot{P}^t_{Ki} = Q^t_{f_{Ki}} \quad (15)$$

where M_{fk} is the lumped fluid mass of node K, $\dot{u}^t_{Ki}$ is component i of the fluid acceleration at node K, $F^t_{f_{Ki}}$ is component i of the fluid forces at node K, V_{fk} is the lumped fluid volume at node K, $\dot{P}^t_{Ki}$ is component i of the fluid pressure rate at node K and $Q^t_{f_{Ki}}$ is component i of the fluid pressure fluxes at node K. Those equations are integrated using the trapezoidal rule along with an explicit solution procedure to yield the nodal fluid velocity and pressure:

$$u^t_{Kj} = u^{t-\Delta t}_{Kj} + 0.5\,\Delta t\,(\dot{u}^t_{Kj} + \dot{u}^{t-\Delta t}_{Kj}) \quad (16)$$

$$P^t_{Kj} = P^{t-\Delta t}_{Kj} + 0.5\,\Delta t\,(\dot{P}^t_{Kj} + \dot{P}^{t-\Delta t}_{Kj}) \quad (17)$$

4. FLUID-STRUCTURE COUPLING MODEL

Newton's equations of motion are used to find a common normal acceleration for the fluid and the solid at the interface. This is done for each node at the fluid-structure boundary as follows:

$$(m_s + m_f)\vec{u}_n = \sum FluidForces + \sum StructureForces \quad (18a)$$

$$(m_s + m_f)\vec{v}_n = \sum FluidForces + \sum StructureForces \quad (18b)$$

where m_s is the solid mass of the node, m_f is the fluid mass of the node, $\vec{u}_n$ and $\vec{v}_n$ are respectively the fluid and solid accelerations of the node normal to the fluid-structure interface. The tangential fluid and solid accelerations $(\vec{u}_t, \vec{v}_t)$ are calculated using the following equations:

$$\left((1-s)m_s + m_f\right)\vec{u}_t = (1-s)\sum StructureForces + \sum FluidForces \quad (19a)$$

$$\left(m_s + (1-s)m_f\right)\vec{v}_t = \sum StructureForces + (1-s)\sum FluidForces \quad (19b)$$

where s is the slip factor. A no-slip condition corresponds to a slip factor of zero. The slip factor determines how much of the fluid and structure forces are mutually exchanged. Equations 18 and 19 are written for all fluid-solid interface nodes. The fluid mesh must move and deform with the tank. This is done by modeling the fluid mesh using very light and compliant (3 orders of magnitude less than the tank) solid brick elements (called "mock" mesh). The ALE formulation is used to account for the fluid mesh deformation/motion.

5. VOF FREE-SURFACE MODEL

For each fluid element a VOF value between 0 and 1 is defined, where 0 corresponds to empty elements and 1 corresponds to elements completely filled with fluid. The elements' VOF values are updated each time-step by moving fluid from a completely or partially filled "donor" element to an empty or partially filled neighboring "acceptor" element using the following model:

$$V_{eo} = V_e\ \mathrm{VOF}_e \quad (20)$$

$$V_{na} = V_n\,(1 - \mathrm{VOF}_n) \quad (21)$$

$$\Delta V = \begin{cases} \Delta t\,S\,A\,\vec{n}.\vec{u} & V_{eo} > \Delta V \ \text{ and } \ V_{na} > V_{eo} \\ V_{eo} & V_{eo} < \Delta V \\ V_{na} & V_{na} < \Delta V \end{cases} \quad (22)$$

where V_e is the volume of the element; V_n is the volume of the neighboring element; V_{eo} is the volume of the element occupied by the fluid; V_{na} is the volume of the neighboring element available to receive fluid; ΔV is the volume flow through the boundary between the two elements in a time step; Δt is the solution time step; S is the surface area between the two elements; A is a value between 0 and 1 indicating the free-surface aperture through which the fluid can move from the element to the neighboring element; $\vec{n}$ is the unit normal to S; and $\vec{u}$ is the fluid velocity vector at the surface S. If ΔV is less than 0 then the element is an acceptor element and the VOF values are not updated because they will be updated later when the neighbor element is set to be the donor element. So if ΔV is greater than 0 then the VOF values are updated using the following equations:

$$\mathrm{VOF}_e = \mathrm{VOF}_e - \Delta V / V_e \quad (23)$$

$$\mathrm{VOF}_n = \mathrm{VOF}_n + \Delta V / V_n \quad (24)$$

The free-surface apertures A at the element interfaces are used to limit the fluid flow based on the location of the free surface

inside the element. A is calculated as follows. If the VOF value of the element is 1 then there is no free-surface at the element, therefore A=1. For elements with a VOF value less than 1, the following steps are used to calculate A:

- Calculate the normal to the surface by looking at a stencil of neighboring elements around the element. This is done using the following equation:

$$n_{e_i} = \mathrm{VOF}_{n_k} S_{n_k} n_{n_{ki}} \quad i=1, 2, 3 \qquad (25)$$

where n_{e_i} is i^{th} component of the normal to the free-surface at the element, VOF_{n_k} is the VOF value for neighboring element number k, S_{n_k} is the area of the intersection surface between the element and neighboring element k, and $n_{n_{ki}}$ is the component i of the normal to the surface between the element and neighboring element k. $\vec{n}_e$ is then normalized into a unit vector. Figure 1 shows a 2D 4-node quadrilateral and the free-surface along with the normal $\vec{n}_e$.

- Calculate the apertures A for each neighboring element by constructing a planar surface with normal $\vec{n}_e$ and with total volume equal to $\mathrm{VOF}_e V_e$ (see Figure 1).

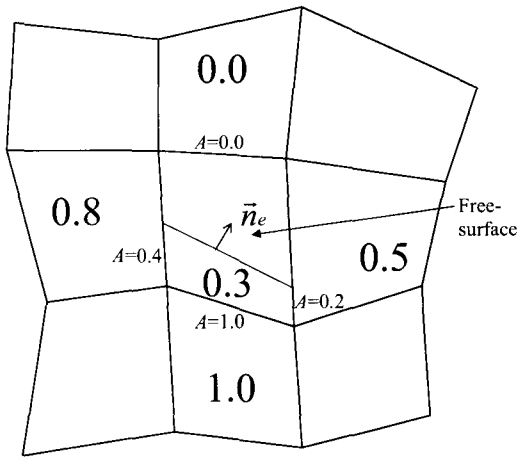

Figure 1 Stencil of neighboring elements used to determine the free-surface normal $\vec{n}_e$ and the liquid free-surface.

6. EXPLICIT SOLUTION PROCEDURE

The solution fields for modeling the solid, fluid and liquid free-surface are defined at the model nodes. These are:

- Solid translational positions.
- Solid translational velocities.
- Solid translational accelerations.
- Solid rotation matrices.
- Solid rotational velocities.
- Solid rotational accelerations.
- Fluid velocities.
- Fluid accelerations.
- Fluid pressure.
- Fluid pressure rate.
- Volume-of-fluid.
- In addition, eddy kinetic energy and eddy kinetic energy rate can be added to model turbulence if an LES turbulence model is used.

The explicit time integration solution procedure for modeling the coupled response of the solid (multibody system), fluid, and liquid free-surface (using the VOF formulation) predicts the time evolution of the above response quantities. The procedure is implemented in the DIS [27] (Dynamic Interactions Simulator) commercial software code and is outlined below:

1- Prepare the run:
   a. Set the initial conditions for the solution fields identified above.
   b. Create a list of all the finite elements (including both solid and fluid elements).
   c. Create a list of elements that will run on each processor. This is done using an algorithm which tries to make the computational cost on each processor equal.
   d. Create a list of all the constraints (including both solid and fluid constraints).
   e. Calculate the solid masses for each finite element node by looping through the list of finite elements. Note that the solid masses are fixed in time.
   f. For each node create a list of corner and edge nodes that are connected to it using fluid volume elements.
   g. VOF preparations:
      i. Find a list of the volume fluid elements.
      ii. Create a list of fluid volume elements that will run on each processor. This is done using an algorithm which tries to make the computational cost on each processor equal.
      iii. For each element find all neighboring elements.
      iv. For each element find the element VOF using the nodal VOF.
      v. Re-interpolate the elements' VOF to nodal VOF.
   h. Loop over all the elements and find the minimum time step for the explicit solution procedure.
   i. Loop over all the elements and create a list of wall nodes. For each wall node find the list of fluid boundary elements.

2- Loop over the solution time and increment the time by Δt each step while doing the following:
   a. Set the nodal values at the last time step to be equal to the current nodal values for all solution fields.
   b. Do 2 iterations (a predictor iteration and a corrector iteration) of the following:
      i. Initialize the nodal fluxes to zero. Those include: solid forces, solid moments, fluid forces, boundary fluid forces, and pressure fluxes. In addition, the lumped nodal fluid volume and fluid mass vectors are also initialized to zero.
      ii. Calculate the nodal solid and fluid fluxes and the lumped fluid volume/mass vectors by looping through all the elements while calculating and assembling the element nodal fluxes and vectors. This is the most computational intensive step. This step is done in parallel by running each list of elements identified in step 1.c on one processor.
      iii. Find the nodal values at the current time step using the semi-discrete equations of motion and the trapezoidal time integration rule (Equations 1-5 and 14-17).
      iv. Execute the solid and fluid constraints. The constraints set the nodal value(s) to prescribed values.
      v. Apply fluid-structure interface boundary conditions for all wall nodes found in Step 1.i (see Equations 18, 19). This is done by doing the following for each wall node:

1. Find the normal to the surface at the wall node.
2. Normalize the surface normal.
3. Find the solid, fluid bulk and fluid boundary forces in the directions normal and tangent to the surface.
4. Find the normal and tangential solid and fluid accelerations using the trapezoidal integration rule and the wall slip percentage.

vi. Set the pressure boundary conditions at the free surface.

vii. Update the VOF field:
1. For each fluid element calculate the element volume. This step is done in parallel using the list of fluid elements for each processor found in Step 1.g.ii.
2. For each fluid element find the apertures through which the fluid convects to each neighboring element. This step is done in parallel using the list of fluid elements for each processor found in Step 1.g.ii.
3. For each fluid element use the apertures, the element volume, the element current VOF value, and the element nodal velocities to update the VOF value of all neighboring elements by finding the volume of fluid that left the element during that time step using Equations 20-24. This step is done in parallel using the list of fluid elements for each processor found in Step 1.g.ii. Note that this step depends on the order of the elements in the list of elements. However, since the updates of the VOF field between solution time steps are small, therefore this dependence is generally very small. In order to assure minimum dependence on the elements' order, at a time step the elements are updated from first to last, then at the next time step they are updated from last to first.

viii. Average the fluid pressure (This step eliminates the pressure checker-boarding effect and allows use of equal order interpolation for both pressure and velocity).

ix. Go to the beginning of step 2.

An advantage of explicit solution procedures is that they are "embarrassingly" parallel. The above procedure achieves near linear speed-up with the number of processors.

7. NUMERICAL SIMULATIONS

Figure 2 shows snapshots of liquid sloshing in an oval tank. The liquid modeled is water ($\rho = 1000$ Kg, $\mu = 0.001$ Kg/(m.sec)). The tank dimensions are: 0.324 m length, width 0.428 m and height 0.276 m. The fluid is modeled as incompressible using the artificial compressibility technique with an artificial sound speed factor of 0.1 (i.e. the artificial sound speed in the water is taken as 1483m/sec x 0.1 = 148.3 m/sec). Due to the use of large elements near the solid surface, full slip boundary condition at the wall is used. Thus, the viscous wall friction effects are assumed to be negligible. The liquid starts from the initial conditions at time 0 shown in Figure 2 and then sloshes in the tank under a gravity field in the vertical direction of 9.8 m/sec^2.

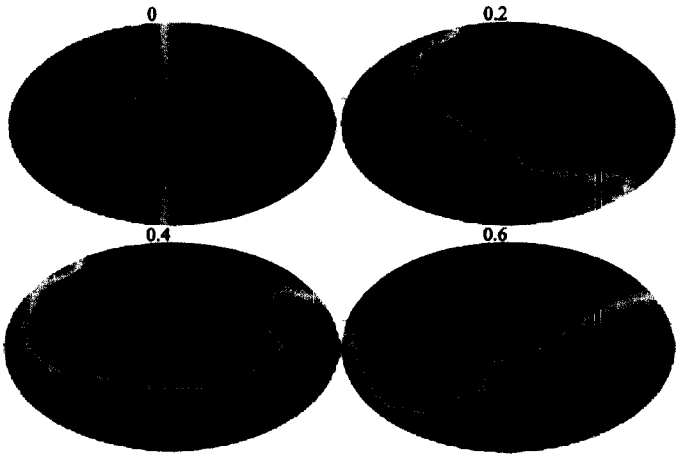

Figure 2 Snapshots of the DIS simulation of liquid sloshing in an oval tank from time 0 to 0.6 sec.

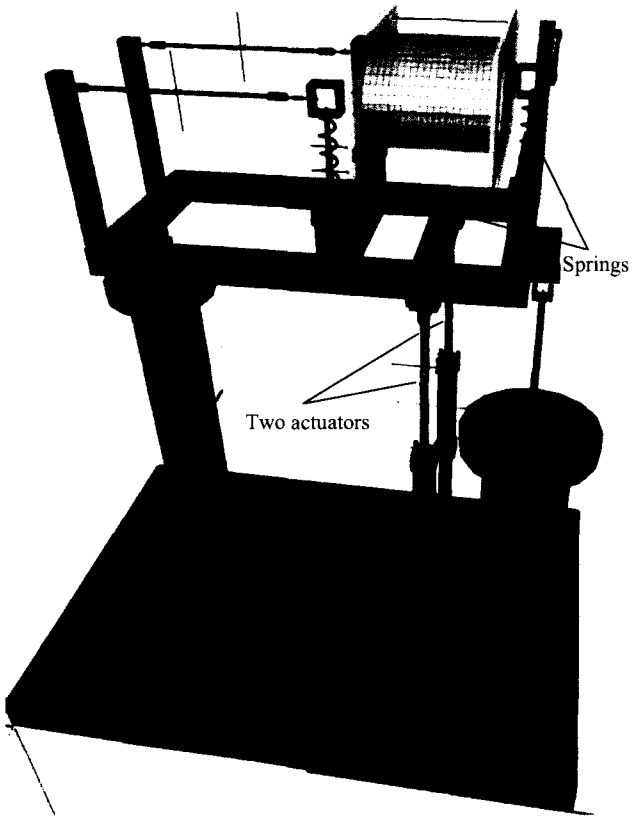

Figure 3 Multibody test fixture with a tank mounted on a suspension system composed of 3 linear springs.

Next the above tank is mounted on a suspension system which is mounted on a test fixture. The test fixture was physically constructed to validate the computational code. Physical experiments to validate the computational code presented in this paper will be conducted in the near future. The test fixture simulates some of the maneuvers that a typical tank in a tanker truck is subjected to such as roll and/or pitch. The test fixture is composed of the following components (Figure 3):

- *Three linear springs*. Simulate the suspension system of the tanker truck.

- *A chassis.* The springs are mounted on the chassis using spherical joints.
- *Two linear actuators* connected to the chassis provide the ability to move the chassis in order to simulate roll, pitch and combined roll/pitch.
- *A rigid grounded base.*
- *Connecting rods.* Provide lateral and longitudinal stability for the tank.
- *17 spherical joints.*
- 5 prismatic joints located at the 3 suspension system springs and the two actuators.
- The tank is assumed to be flexible and is modeled using shell elements.

The same initial conditions as in Figure 2 where tank is half-full and the liquid free-surface is vertical are used as initial conditions for fully coupled multibody-liquid sloshing simulation of the test fixture. Figure 4 shows snapshots of the motion of the test fixture and the liquid from time 0 to 0.75 sec. Figure 5 shows snapshots from different angles taken at time 0.5 sec.

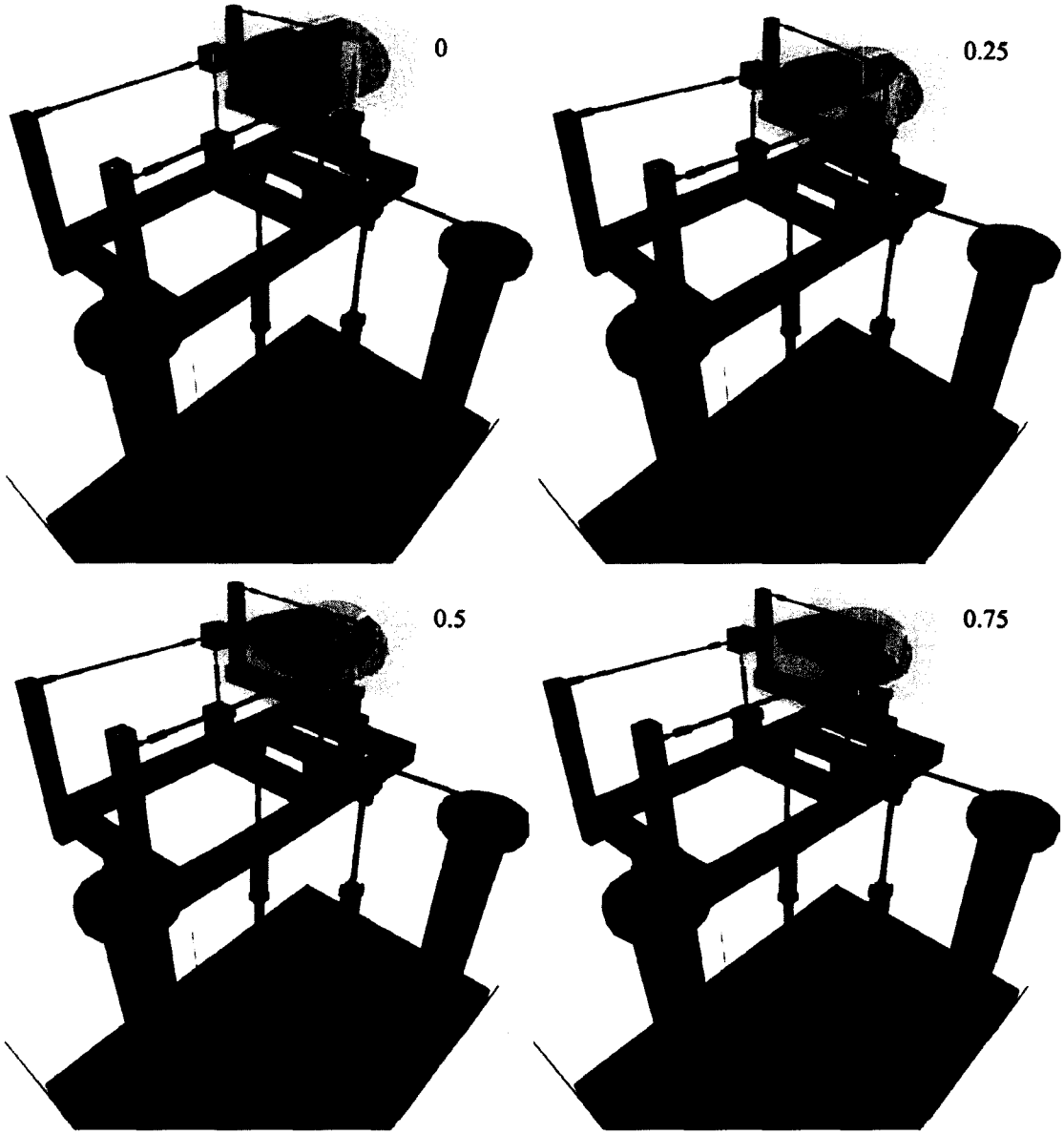

Figure 4 Snapshots of the simulation of the coupled multibody-fluid simulation of liquid sloshing in the oval tank.

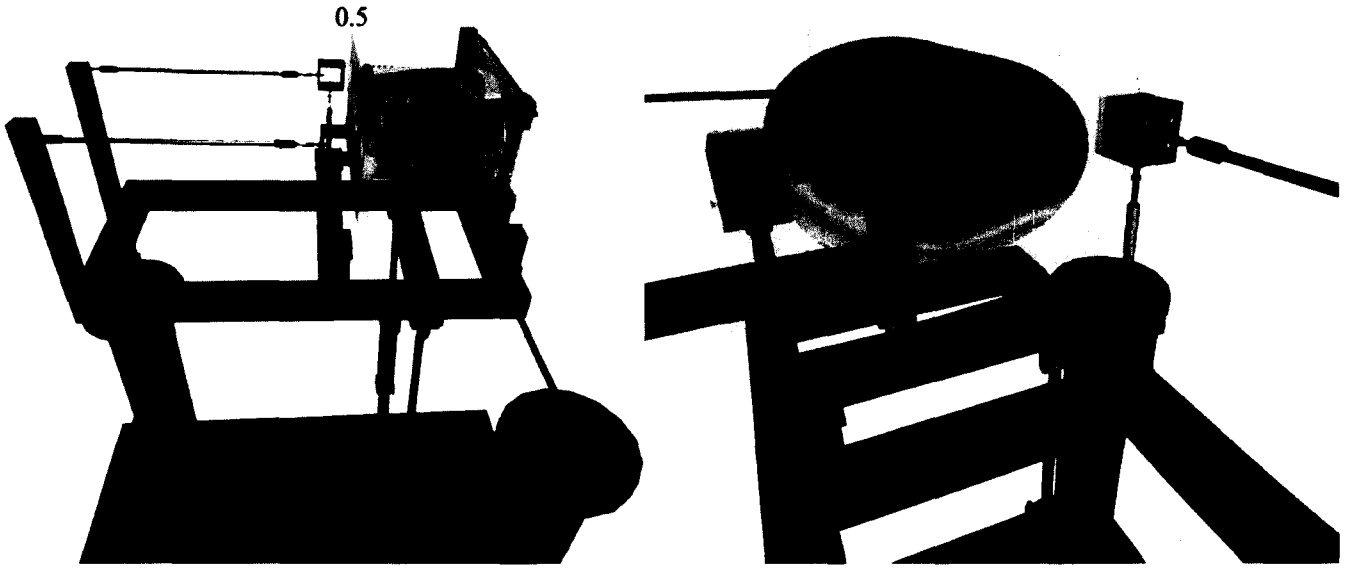

Figure 5 Snapshots of two views the DIS simulation of the test fixture. In the snapshot on the right the tank is colored using pressure.

8. CONCLUDING REMARKS

A finite element model for predicting the fully coupled dynamic response of flexible multibody systems and liquid sloshing in containers was presented. The model has the following characteristics:

- Parallel explicit time-integration solver.
- Library of accurate large rotation finite elements including: truss, beam, shell and solid elements. The elements only use Cartesian coordinates as DOFs.
- The fluid mesh is modeled using a very light and compliant solid mesh which allows the fluid mesh to move/deform along with the tank using the Arbitrary Lagrangian-Eulerian formulation.
- Acceptor-donor VOF algorithm for modeling the fluid's free-surface.
- The motion of the solid and fluid is referred to a global inertial Cartesian reference frame.
- A total Lagrangian deformation description is used for the solid elements.
- The penalty technique is used to model the joints.

Numerical simulations were presented for a half-filled tank supported by linear springs mounted on a test fixture. Physical experiments will be conducted in the near future to validate the computational model presented in this paper.

ACKNOWLEDGEMENTS

Support for this work provided by the US Army TACOM, Warren, MI under SBIR grant number W56HZV-05-C-0117 and by Indiana 21st Century Research and Technology Fund under grant number 0063 is gratefully acknowledged.

REFERENCES

[1] Gerrits, J. and Veldman, A., "Numerical simulation of coupled liquid-solid dynamics," *European Congress on Computation Methods in Applied Science and Engineering*, ECCOMAS 200, Barcelona, 2000.

[2] Fekken, G., "Numerical simulation of a free-surface flow with moving rigid bodies," *Ph.D. Dissertation, University of Groningen*, 2004.

[3] Rumold, W., "Modeling and simulation of vehicles carrying liquid cargo", *Multibody System Dynamics*, Vol 5, pp. 351-374, 2001.

[4] Tezduyar, T.E., "Finite element methods for flow problems with moving boundaries and interfaces," *Archives of Computational Methods in Engineering*, Vol. 8(2), pp. 8-130, 2001.

[5] Walhorn, E., Kolke, A., Hubner, B., and Dinkler, D., "Fluid–structure coupling within a monolithic model involving free surface flows," *Computers and Structures*, Vol. 83, pp. 2100-2111, 2005.

[6] Nomura, T., "ALE finite element computations of fluid-structure interaction problems," Computer Methods in Applied Mechanics and Engineering, Vol. 112(1-4), pp. 291-308, 1994.

[7] Idelsohn, S.R., Onate, E, Del Pin, F. and Calvo, N., "Fluid-structure interaction using the particle finite element method," *Computer Methods in Applied Mechanics and Engineering*, in press, 2005.

[8] Hirt, C.R. and Nichols, B.D., "Volume of fluid (VOF) method for the dynamics of free boundaries," *Journal of Computational Physics*, Vol. 39, pp. 201-225, 1981.

[9] Youngs, D.L., "An interface tracking method for a 3D Eulerian hydrodynamics code," *Technical Report AWRE/44/92/35, Atomic Weapons Research Establishment*, 1987.

[10] Souli, M. and Zolesio, J.P., "Arbitrary Lagrangian-Eulerian and free surface methods in fluid mechanics," *Computer Methods in Applied Mechanics and Engineering*, Vol. 191, pp. 451-466, 2001.

[11] Braess, H. and Wriggers, P., "Arbitrary Lagrangian Eulerian finite element analysis of free surface flows," *Computer Methods in Applied Mechanics and Engineering*, Vol. 190, pp. 95-109, 2000.

[12] Stein, K. and Tezduyar, T., "Advanced mesh update techniques for problems involving large displacements," *Fifth world congress on computation mechanics*, WCCM V, Vienna, Austria, 2002.

[13] Bilarbegian, M. and Zu, J.W., "Dynamic analysis and simulation of vehicles carrying liquids during braking," ASME DETC2005-85102, *5th International Conference on Multibody Systems, Nonlinear Dynamics, and Control*, ASME DETC, Long Beach, CA, 2005.

[14] Wasfy, T.M. and Noor, A.K., "Computational Strategies for Flexible Multibody Systems," *Applied Mechanics Reviews,* 56(6), 553-613, 2003.

[15] Wasfy, T.M. and Noor, A.K., "Modeling and sensitivity analysis of multibody systems using new solid, shell and beam elements," *Computer Methods in Applied Mechanics and Engineering*, Vol. 138(1-4) (25th Anniversary Issue), pp. 187-211, 1996.

[16] Wasfy, T.M., "A torsional spring-like beam element for the dynamic analysis of flexible multibody systems," *International Journal for Numerical Methods in Engineering*, Vol. 39(7), pp. 1079-1096, 1996.

[17] Wasfy, T.M., "Edge projected planar rectangular element for modeling flexible multibody systems," 19th Biennial Conference on Mechanical Vibration and Noise, Paper No. DETC2003-48351, *19th Biennial Conference on Mechanical Vibration and Noise*, ASME International 2003 DETC, Chicago, IL, 2003.

[18] Wasfy, T.M., "Lumped-parameters brick element for modeling shell flexible multibody systems," *18th Biennial Conference on Mechanical Vibration and Noise*, ASME International 2001 DETC, Pittsburgh, PA, 2001.

[19] Wasfy, T.M., "Modeling spatial rigid multibody systems using an explicit-time integration finite element solver and a penalty formulation," ASME Paper No. DETC2004-57352, *28th Biennial Mechanisms and Robotics Conference*, DETC, Salt Lake, Utah 2004.

[20] Leamy, M.J. and Wasfy, T.M., "Transient and steady-state dynamic finite element modeling of belt-drives," *ASME Journal of Dynamics Systems, Measurement, and Control*, Vol. 124(4), pp. 575-581, 2002.

[21] Wasfy, T.M. and Leamy, M.J., "Modeling the dynamic frictional contact of tires using an explicit finite element code," ASME DETC2005-84694, *5th International Conference on Multibody Systems, Nonlinear Dynamics, and Control*, ASME DETC, Long Beach, CA, 2005.

[22] Wasfy, T.M., "Asperity spring friction model with application to belt-drives," Paper No. DETC2003-48343, Proceeding of the DETC: *19th Biennial Conference on Mechanical Vibration and Noise*, Chicago, IL, 2003.

[23] Wasfy, T.M. and Leamy, M.J., "Dynamic modeling of synchronous belt-drives using an explicit finite element code," ASME DETC2005-85103, *5th International Conference on Multibody Systems, Nonlinear Dynamics, and Control*, ASME DETC, Long Beach, CA, 2005.

[24] Meckstroth, R.J., Wasfy, T.M., and Leamy, M.J., "Finite element study of the dynamic response of serpentine belt-drives with isolator clutches," *SAE 2004 Congress*, Paper No. 2004-01-1347, Detroit, MI, 2004.

[25] Chorin, A.J., "A Numerical Method for Solving Incompressible Viscous Flow Problems," *Journal of Computational Physics*, Vol. 2(1), 1967.

[26] Wasfy, T.M., West, A.C. and Modi, V., "Parallel finite element computations of unsteady incompressible flows," *International Journal for Numerical Methods in Fluids*, Vol. 26(1), pp. 17-37, 1998

[27] DIS (Dynamic Interactions Simulator), http://www.ascience.com/ScProducts.htm, Advanced Science and Automation Corp., 2006.